

# Single-walled carbon nanotubes-ciprofloxacin nanoantibiotic: strategy to improve ciprofloxacin antibacterial activity

Mohyeddin Assali<sup>1</sup>  
Abdel Naser Zaid<sup>1</sup>  
Farah Abdallah<sup>1</sup>  
Motasem Almasri<sup>2</sup>  
Rasha Khayyat<sup>3</sup>

<sup>1</sup>Department of Pharmacy, Faculty of Medicine and Health Sciences, An Najah National University, Nablus, Palestine; <sup>2</sup>Department of Biology and Biotechnology, Faculty of Science, An Najah National University, Nablus, Palestine; <sup>3</sup>Department of Biomedical Sciences, Faculty of Medicine and Health Sciences, An Najah National University, Nablus, Palestine

**Abstract:** As infectious diseases continue to be one of the greatest health challenges worldwide, the demand toward alternative agents is continuously increasing. Recent advancement in nano-technology has expanded our ability to design and construct nanomaterials to treat bacterial infections. Carbon nanotubes are one among these nanomaterials. Herein, we describe the covalent functionalization of the single-walled carbon nanotubes (SWCNTs) with multiple molecules of ciprofloxacin. The prepared nanoantibiotics were characterized using different techniques, including transmission electron microscopy, Raman spectroscopy, and thermogravimetric analysis. The characterization of the nanoantibiotics confirmed the successful covalent functionalization of the SWCNTs with 55% of functionalization as has been observed by thermogravimetric analysis. The release profile revealed that 90% of the loaded ciprofloxacin was released within 2.5 h at pH 7.4 showing a first-order release profile with  $R^2 > 0.99$ . Interestingly, the results of the antibacterial activity indicated that the functionalized SWCNTs have significant increase in the antibacterial activity against the three strains of bacteria – by 16-fold for *Staphylococcus aureus* and *Pseudomonas aeruginosa* and by 8-fold for *Escherichia coli* – in comparison to the ciprofloxacin free drug. Moreover, the synthesized nanoantibiotic showed high hemocompatibility and cytocompatibility over a wide concentration range.

**Keywords:** covalent functionalization, hydrophilic/hydrophobic balance, carbon nanotubes, nanoantibiotic

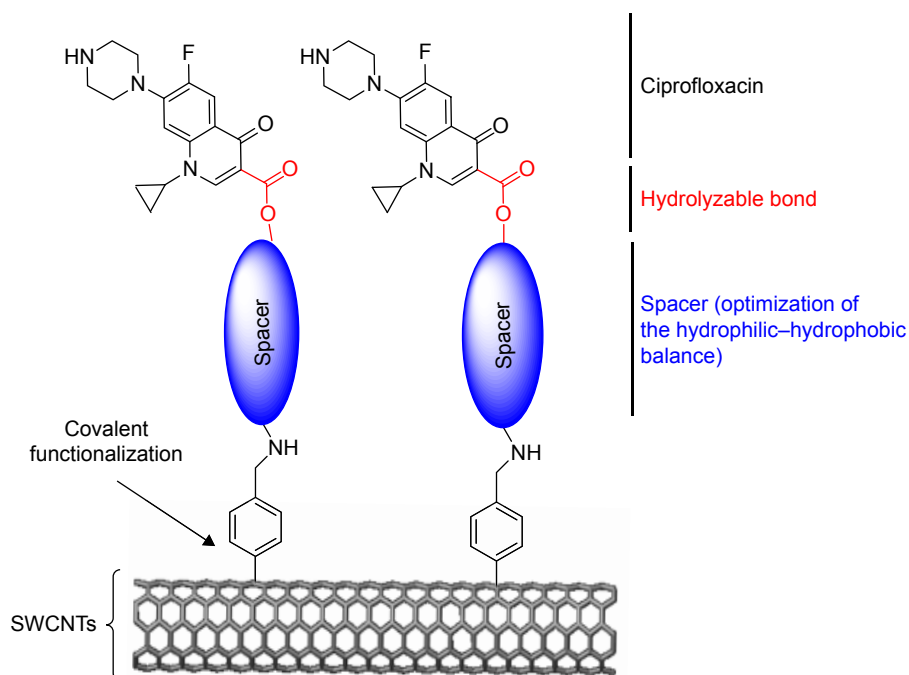
## Introduction

At the beginning of the 20th century, infectious diseases were the leading cause of death worldwide.<sup>1</sup> The decrease in morbidity and mortality from infectious diseases over the last century was attributed mainly to the introduction of antimicrobial agents and antibiotics in the pharmaceutical field. However, due to the intensive use of antibiotics, human pathogens have become resistant to many antibiotics through various types of mutations.<sup>2-5</sup> It is now estimated that multiple drug-resistant bacteria cause ~60% of nosocomial infections.<sup>2</sup> On the other hand, developing completely new antibiotics will not be easy in the present world economic condition. Since antibiotics have a limited lifespan of utility, soon we will reach a point when humans will not be able to confidently treat bacterial infections by using available antibiotics as can be seen from the decreasing number of approved antibiotics by the FDA in the last decades.<sup>6</sup> Thus, there is an urgent need to discover new approaches of antimicrobial agents that can be used to treat antibiotic-resistant strains effectively. One promising method is to use suitable nanomaterials for selective treatment of bacterial infections.<sup>7-9</sup> These nanomaterials possess high surface area to volume ratios and unique chemophysical

Correspondence: Mohyeddin Assali  
Department of Pharmacy, Faculty of  
Medicine and Health Sciences, An Najah  
National University, PO Box 7,  
Nablus, Palestine  
Tel +970 9 234 5113  
Fax +970 9 234 9739  
Email m.d.assali@najah.edu

properties, which contribute to their effective antibacterial activities.<sup>10</sup> Various proposed antibacterial mechanisms involved damaging of the bacterial cell wall/membrane, production of reactive oxygen species that damage bacterial components, interruption of energy transduction, and inhibition of enzyme activity and DNA synthesis.<sup>11</sup> Among nanotechnology-derived materials, carbon nanotubes (CNTs) have stimulated a great interest for biomedical applications because of their unique mechanical, electrical, thermal, and spectroscopic properties.<sup>12–14</sup> It is important to note that recent studies showed that the functionalization of CNTs with different approaches increase the biocompatibility and decrease toxicity.<sup>15–18</sup> Among these studies, Guo et al studied the *in vivo* toxicity of functionalized multi-walled carbon nanotubes (*f*-MWCNTs) in mice. The MWCNTs were functionalized with glucosamine and labeled with radioisotopes technetium-99 (<sup>99m</sup>Tc-MWNT-G), and the results showed that no severe acute toxicity responses were observed.<sup>15</sup> In another study, Liu et al detected the *in vivo* toxicity and excretion of single-walled carbon nanotubes (SWCNTs) in mice by Raman spectroscopy. Functionalized SWCNTs (*f*-SWCNTs) by branched polyethylene-glycol (PEG) chains were injected intravenously. The *f*-SWCNTs were detected in the intestine, feces, kidney, and bladder of mice, and the excretion was via the biliary and renal pathways with no toxic side effects of SWCNTs to mice were observed.<sup>16</sup>

With their biocompatibility, CNTs possess high carrying capacity which can load various copies of different ligands at the same time.<sup>19,20</sup> Ciprofloxacin is considered to be one of the most effective antibiotics of the fluoroquinolones, and it is currently used for the treatment of many types of infections.<sup>21–24</sup> Its mechanism of action involves the inhibition of topoisomerase II (DNA gyrase) and topoisomerase IV, which are essential for the replication, transcription, and repair of bacterial DNA.<sup>25</sup> However, it is classified as class IV (low water solubility and intestinal permeability) according to biopharmaceutical classification system.<sup>26</sup> Because of its wide use in numerous clinical conditions, resistant strains began to emerge. The mechanism of resistance includes either one or more point mutations in the quinolone binding region of the target enzyme or change in the permeability of the organism due to the efflux pump effect.<sup>27</sup> So, herein we aim to develop, for the first time, a new nanoantibiotic based on covalent functionalization of SWCNTs with multiple molecules of ciprofloxacin. Moreover, the large surface area of SWCNTs permits the multiple loading of the ciprofloxacin, and various nanotubes will be exposed and aggregate with the bacteria strains. Moreover, different derivatives of PEG spacers were used in order to enhance the aqueous solubility of the formed nanoconjugate connected to ciprofloxacin through hydrolyzable ester bond as shown in Scheme 1. The ester prodrug strategy is an excellent strategy that used to



**Scheme 1** General scheme that describes the covalent functionalization of SWCNTs with ciprofloxacin.

**Abbreviation:** SWCNTs, single-walled carbon nanotubes.

release the active drug by the carboxylesterase enzyme in the tissues as it is found in much more concentration in the tissues in comparison to the red blood cells (RBCs) and the plasma as documented in the literature.<sup>28–30</sup>

## Materials and methods

### Reagents and instrumentation

All materials were used as received and used without further purification. Esterase from porcine liver was purchased from Sigma-Aldrich Company, Spectra/Por® 4 dialysis membrane (12–14 kD MWCO, 25 mm flat width, 100 ft length) was purchased from Spectrum Laboratories, Inc Company (Rancho Dominguez, CA, USA). Dulbecco's Modified Eagle's Medium (DMEM) and L-glutamine solution were purchased from Biological industries (Cromwell, CT, USA). Trypsin-EDTA solution and calf serum, iron-fortified were purchased from Sigma-Aldrich (St Louis, MO, USA). Celltiter 96® Aqueous one solution cell proliferation assay (MTS) was purchased from Promega (Madison, WI, USA). All reactions were stirred under ambient conditions using, as received, solvents and dried glassware, unless it was mentioned elsewhere. Column chromatography was conducted using silica gel (pore size 60 Å, particle size 40–63 µm, 230–400 mesh particle size, Sigma Aldrich Company) in order to purify the products. Nuclear Magnetic Resonance (NMR) spectra were recorded with Bruker Avance 300 MHz spectrometer (Bruker, Zurich, Switzerland). Chemical shifts were reported in ppm, and coupling constants were reported in Hz. Ultraviolet–visible (UV–Vis) spectra were recorded with 7315 Spectrophotometer (Jenway, Staffordshire, UK), using quartz cuvettes. Raman spectra were recorded on a LabRAM HR High-Resolution 800 UV Confocal Raman microscope, and the measurements were realized with green laser He-Ne 532.14 nm, 600 line/mm, 20× objective, 20 mW, pinhole 100 µm. Thermogravimetric analysis (TGA) spectra were recorded by STA 409 PC Luxx®, (NETZSCH) in the range 0°C–800°C, with a heating rate of 20°C/min, under nitrogen (100 cc/min). Transmission electron microscopy (TEM) images were taken by using Morgagni 286 transmission microscope (FEI Company, Eindhoven, the Netherlands) at 60 kV. The samples (20 µL) were deposited over copper grids covered with carbon films, using uranyl acetate 2% as negative stain.

### Synthesis and functionalization of SWCNTs

A detailed synthesis of compounds **1**, **2**, **3**, **4**, **9**, and **10** can be found in the Supplementary materials.

### Functionalization of SWCNTs with 4-[(N-Boc)aminomethyl]aniline (**5**)

To SWCNTs (32.0 mg) and compound **4** (150.0 mg, 0.68 mmol) dried under vacuum and argon, 20 mL of *o*-dichlorobenzene (DCB) and 10 mL of acetonitrile were added. The reaction was sonicated in water bath for 10 min and was put in a stirrer. After bubbling with argon, 0.50 mL of isoamyl nitrite was added dropwise. The reaction mixture was stirred and heated at 60°C for 19 h under argon. After cooling the reaction to room temperature, unfunctionalized SWCNTs were removed by low-speed centrifugation at 3,000 rpm for 10 min. Then, the functionalized SWCNTs were washed with 40 mL of MeOH twice, 25 mL of dichloromethane (DCM), 20 mL of dimethylformamide, and (2×20 mL) of diethyl ether. The resulting black solid product was dried under vacuum. Weight of the product was 25 mg.

### Deprotection of Boc group from *f*-SWCNTs **5** (**6**)

A measured quantity of 4 mL of trifluoroacetic acid (TFA) was added to solution of *f*-SWCNTs **5** (25 mg) in 6 mL of DCM sonicated for 5 min. The reaction was stirred for 24 h at room temperature. The solvent was removed under vacuum. Then, 20 mL of MeOH was added, sonicated for 5 min, and centrifuged at 3,000 rpm for 10 min. The washing process was repeated with another 20 mL of MeOH and (2×20 mL) of diethyl ether. The resulting black solid product was dried under vacuum. The obtained weight was 20.0 mg. The quantitative Kaiser test was used to determine the amount of free-loaded NH<sub>2</sub>, as described previously.<sup>31</sup>

### Attachment of compound **3** on *f*-SWCNTs **6** (**7**)

A measured quantity of 10 mL of DCM was added to compound **3** (70.0 mg, 0.11 mmol), *f*-SWCNTs **6** (10 mg), EDC (66.0 mg, 0.33 mmol), and N,N-diisopropylethylamine (DIPEA) (25 µL, 0.17 mmol) that were dried under vacuum and N<sub>2</sub>. The reaction mixture was run overnight at room temperature. Fifteen milliliters of MeOH was added after the evaporation of solvent. The reaction mixture was sonicated for 5 min and centrifuged at 15,000 rpm for 10 min. After that the supernatant was taken, and the washing process was repeated with another 15 mL of MeOH and (2×15 mL) of diethyl ether. The resulting black solid product was dried under vacuum.

### Deprotection of Boc group in *f*-SWCNTs **7** (**8**)

A measured quantity of 4 mL of TFA was added to solution of *f*-SWCNTs **7** (30.0 mg) in 4 mL of DCM that was sonicated for 5 min. The reaction mixture was stirred overnight at

room temperature. The solvent was removed under vacuum. Then, 20 mL of MeOH was added, sonicated for 5 min, and centrifuged at 3,000 rpm for 10 min. The washing process was repeated with another 20 mL of MeOH and (2×20 mL) of diethyl ether. The resulting black solid product was dried under vacuum. The obtained weight was 22.0 mg.

#### Attachment of compound **10** on *f*-SWCNTs **6** (**11**)

To compound **10** (80.0 mg, 0.11 mmol), *f*-SWCNTs **6** (10 mg), EDC (66.0 mg, 0.34 mmol), and DIPEA (30  $\mu$ L, 0.17 mmol), 10 mL of dry DCM was added. The reaction was run overnight at room temperature under argon. Fifteen milliliters of MeOH was added after the evaporation of solvent. The reaction mixture was sonicated for 5 min and centrifuged at 15,000 rpm for 10 min. After the supernatant was taken, the washing process was repeated with another 15 mL of MeOH and (2×15 mL) of diethyl ether. The resulting black solid product was dried under vacuum.

#### Deprotection of Boc group in *f*-SWCNTs **11** (**12**)

A measured quantity of 4 mL of TFA was added to solution of *f*-SWCNTs **11** (30.0 mg) in 4 mL of DCM that was sonicated for 5 min. The reaction was run for 24 h at room temperature. The solvent was removed under vacuum. Then, 20 mL of MeOH was added, sonicated for 5 min, and centrifuged at 3,000 rpm for 10 min. The washing process was repeated with another 20 mL of MeOH and (2×20 mL) of diethyl ether. The resulting black solid product was dried under vacuum. The obtained weight was 25.0 mg.

### In vitro drug release

Ciprofloxacin release from SWCNTs was carried out using dialysis membrane in order to evaluate the kinetic of release profile. This was achieved using dialysis bag diffusion technique in PBS. Briefly, *f*-SWCNTs **12** (1.0 mg that contains 55.0  $\mu$ g of ciprofloxacin) and porcine liver esterase (PLE) 10 U/mL were dissolved in 5 mL of freshly prepared PBS solution and transferred to the dialysis bag. The filled bag was immersed in 200 mL of the buffer solution at pH 7.4 and gently stirred for 24 h at 37°C. An aliquot was withdrawn from the release medium at each specified time period and was replaced with an equal volume of fresh medium to mimic the sink conditions of the human blood circulation. The absorbance of the collected samples was measured at  $\lambda_{\text{max}}$  280 nm. Dialysis membrane method was performed in triplicate. The concentrations of the released drug and, subsequently, the percentage of released drug were calculated by compensation of absorbance values in calibration

curve equation of ciprofloxacin. Moreover, standard kinetics models were used in order to determine the release pattern of ciprofloxacin from the nanoantibiotic. The linear regression ( $R^2$ ) and Akaike Information Criterion (AIC) were calculated using DDSolver, an Excel-plugin module.<sup>32</sup>

### Antibacterial activity

The antibacterial activity of *f*-SWCNTs **12** was studied against *Escherichia coli* (ATCC 25922), *Staphylococcus aureus* (ATCC 25923), and *Pseudomonas aeruginosa* (ATCC 27853) strains and compared to the activity of ciprofloxacin and pristine SWCNT (*p*-SWCNTs) alone. Bacterial culture preparation was adjusted using the turbidity of bacterial suspensions according to the 0.5 McFarland standard solution that represent  $1.5 \times 10^8$  CFU/mL.

#### Disc diffusion method

This method was used as a primary technique to determine the antibacterial susceptibility of *f*-SWCNTs **12**, ciprofloxacin, and *p*-SWCNTs. In this method, small filter paper discs dipped in 20  $\mu$ L of *f*-SWCNTs **12** (55  $\mu$ g/mL per 1 mg/mL of *f*-SWCNTs **12**), ciprofloxacin (55  $\mu$ g/mL), and *p*-SWCNTs (1 mg/mL) were put on Mueller Hinton agar plates. After the drying of the discs, the plates were incubated at 35°C for 18 h. Then, the diameters of the zones of inhibition for each sample were measured to obtain the antibacterial activity.

#### Broth microdilution method

This technique was used to determine the minimum inhibitory concentration (MIC) of each compound. The used protocol was conducted according to that of Clinical and Laboratory Standards Institute (CLSI).<sup>33,34</sup> Briefly, ciprofloxacin was dissolved in 100% dimethyl sulfoxide (DMSO) to obtain a concentration of 8  $\mu$ g/mL for *S. aureus* and *P. aeruginosa* and a concentration of 2  $\mu$ g/mL for *E. coli*. While for *f*-SWCNTs **12** and *p*-SWCNTs, they were dissolved in distilled water to achieve a concentration of 8  $\mu$ g/mL per 146  $\mu$ g/mL of *f*-SWCNTs **12** and 146  $\mu$ g/mL, respectively, for *S. aureus* and *P. aeruginosa* and a concentration of 2  $\mu$ g/mL per 36.5  $\mu$ g/mL of *f*-SWCNTs **12** and 36.5  $\mu$ g/mL for *E. coli*. These solutions were serially diluted (twofold) 11 times with BBL Muller Hinton II. In order to detect the presence of antibacterial activity for DMSO in broth microdilution method conditions, 100% DMSO was serially diluted (twofold) with Muller Hinton broth to achieve concentrations from 0.098% to 50%. Then, overnight grown bacterial isolates were applied to all wells except negative control to obtain final bacterial concentration of  $5 \times 10^5$  CFU/mL in each well.



After inoculation of bacteria, the plates were incubated for 18 h at 35°C. Broth microdilution method was performed in duplicate for each isolate. MIC was considered to be the lowest concentration that did not show any visible growth in the test media. MIC was detected by the absorbance of each plate taken at  $\lambda_{\text{max}}$  630 nm for all strains by Stat Fax® 2100-Microplate reader (Awareness Technology INC, Palm City, FL, USA), using Muller Hinton broth as the blank.

## Cellular cytotoxicity

HeLa cell and human hepatic stellate cell (LX-2) were cultured in 15 cm<sup>2</sup> plastic culture plate in culture growth medium (CGM), which consists of DMEM medium supplemented with 10% fetal bovine serum, L-glutamine, and penicillin/streptomycin. Cells were maintained in the above medium at 37°C in a humidified atmosphere containing 5% CO<sub>2</sub>.

For subculturing, the CGM was suctioned from 15 cm<sup>2</sup> culture plate. Then, the cells were washed with 15 mL of Ca<sup>2+</sup>-free PBS. After that, 5 mL of trypsin was added to cells and were incubated for 3 min in a humidified atmosphere containing 5% CO<sub>2</sub> at 37°C until sufficient cells detached from the surface of the plates. After that, trypsin was inactivated by 20 mL of CGM, and subsequently, the cell suspension was collected, diluted, and distributed into a 96-well plate or 12-well plate (according to the test) and were left to adhere over 24 h.

The cells were subcultured into 96-well plate as explained previously. After 24 h, the cells were incubated with 100 µL of different concentrations of the nanoantibiotic for 24 h. Twenty microliters of MTS solution was added to each well followed by an incubation period of 1 h before the absorbance was measured at 490 nm by a plate reader.

## Hemolysis test

Hemolysis test was performed on fresh human blood stabilized with heparin. The test was conducted according to the literature.<sup>35</sup> The human RBCs were centrifuged at 1,000 rpm for 20 min at 4°C and washed five times with PBS (pH = 7.4). Then the collected RBCs were diluted with PBS 10 times. Positive and negative controls were prepared by adding 1 mL of water on 0.1 mL of the diluted RBCs (complete hemolysis) and 1 mL of PBS buffer (no hemolysis), respectively. Sample solutions were prepared by adding various concentrations of the nanoantibiotic on the diluted RBCs in triplicate. After that, the mixtures were incubated for 2 and 24 h and centrifuged at 5,000 rpm for 1 min. The absorption at 541 nm was recorded for each concentration and the hemolysis percentage was calculated according to the following formula:

$$\% \text{ hemolysis} = \frac{\text{Abs of sample} - \text{Abs of negative}}{\text{Abs of positive} - \text{Abs of negative}} \times 100$$

Percentage <10% is considered safe with no hemolytic activity according to the literature.<sup>35</sup>

## Results and discussion

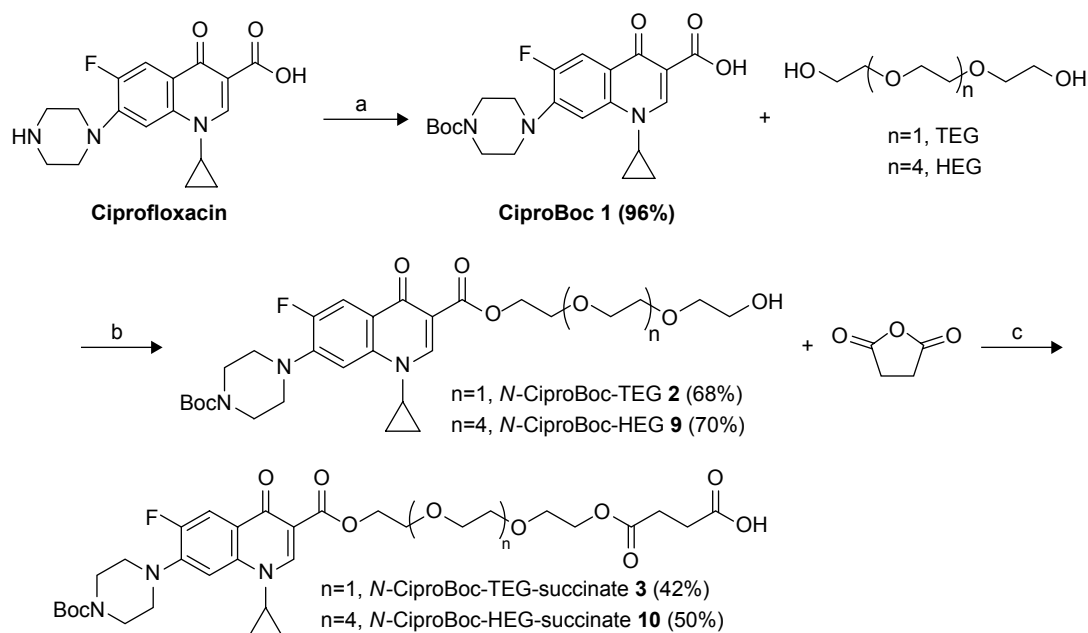
The main strategy is to functionalize the SWCNTs covalently with ciprofloxacin by the support of a spacer to improve the hydrophilic–hydrophobic balance and to obtain a new stable nanoantibiotic. Therefore, we hypothesized the utilization of PEG derivatives starting with triethylene glycol (TEG) as a linker between the ciprofloxacin and the SWCNTs. In the first place, the amine group of ciprofloxacin was protected using Boc group followed by an esterification reaction with the TEG using EDC as a coupling agent and 4-dimethylaminopyridine (DMAP) as a catalyst to form *N*-CiproBoc-TEG **2**. After that, compound **2** was reacted with succinic anhydride using Et<sub>3</sub>N as Hunig's base to form the terminal carboxyl group **3** as shown in Scheme 2.

SWCNTs were covalently functionalized using the diazonium salt arylation reaction. The arylation of SWCNTs with diazonium salts is an efficient method for the functionalization of CNTs, originally developed by the group of Tour.<sup>36</sup> *p*-SWCNTs were functionalized with 4-[(*N*-Boc)aminomethyl]aniline. The resulting derivative was deprotected in acid media as shown in Scheme 3. The corresponding amine loading value was determined by Kaiser test.<sup>37</sup> The total loaded amine was 0.45 mmol/g.

The introduction of *N*-Boc-Cipro-TEG-succinate **3** on the surface of SWCNTs **6** was conducted using EDC as a coupling agent and DIPEA as Hunig's base in order to obtain compound **7**. Then, compound **7** was subjected to a deprotection of Boc group using TFA in order to achieve SWCNTs functionalized with ciprofloxacin as shown in Scheme 4.

Once the successful functionalization of SWCNTs was achieved, its water dispersibility was tested. Unfortunately, the water dispersibility of the *f*-SWCNTs **8** was very low; this can be explained as the length of the spacer is insufficient to get the adequate hydrophilic/hydrophobic balance. Accordingly, an increase in the length of the hydrophilic linker using hexaethylene glycol (HEG) instead of TEG could be beneficial to improve its water solubility.

Following the same synthetic strategy, Cipro-Boc **1** was reacted with HEG to form *N*-Cipro-Boc-HEG **9** in a good yield followed by the reaction with succinic anhydride to produce *N*-Cipro-Boc-HEG-succinate **10**. The functionalized SWCNTs with the terminal amine group were reacted with



**Scheme 2** Synthesis of *N*-CiproBoc-TEG-succinate **3** and *N*-CiproBoc-HEG-succinate **10**. (a) Di-*t*-butyl dicarbonate, sodium hydroxide, water: Dioxane (1:1), 96%; (b) 1-(3-dimethylaminopropyl)-3-ethylcarbodiimide, dimethylaminopyridine, dichloromethane, 20 h; and (c) triethylamine, dichloromethane, 12 h.

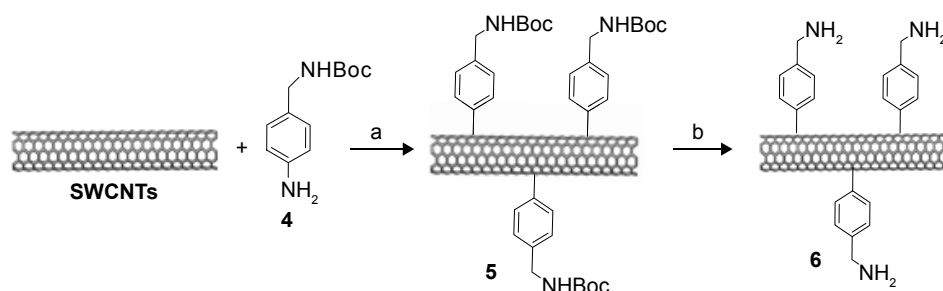
**Abbreviations:** HEG, hexaethylene glycol; TEG, triethylene glycol.

the synthesized compound **10** followed by the deprotection of the Boc group to produce the SWCNTs functionalized with ciprofloxacin with a longer hydrophilic chain as shown in Scheme 4.

After the successful functionalization of SWCNTs with the Cipro-HEG, its dispersibility in water was examined. The *f*-SWCNTs **12** showed good water dispersibility with a physical stability for more than 6 months in comparison to *p*-SWCNTs and *f*-SWCNTs **8** as shown in the inset in Figure 1. Moreover, there was a good chemical stability at the physiological pH (PBS, pH=7.4) with excellent dispersibility. The observation of this stable black suspension is due to the change in the native hydrophobic characteristics of the nanotube side wall, which became more hydrophilic after functionalization of the SWCNTs surface with longer hydrophilic linkers like HEG. Whereas, the *p*-SWCNTs

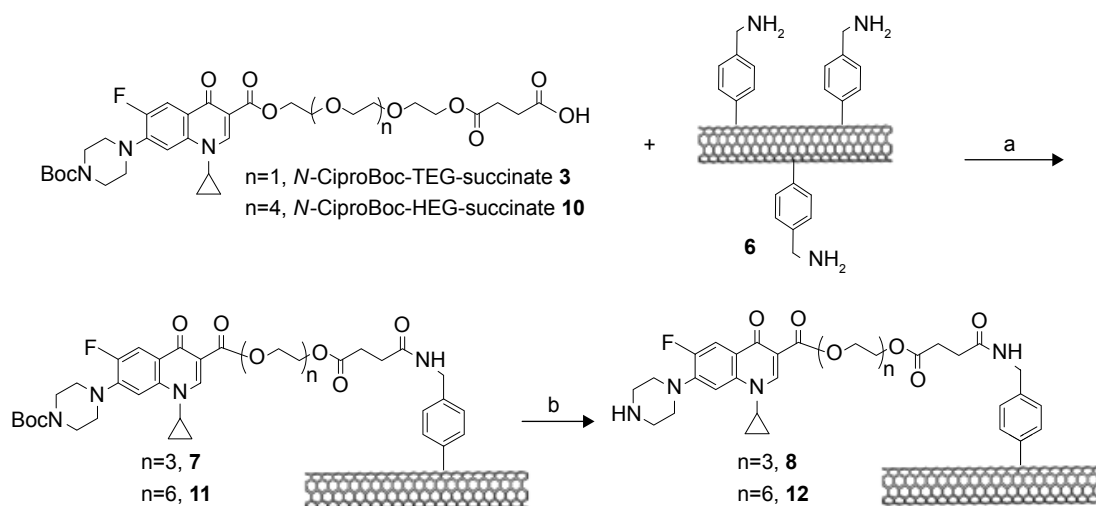
and *f*-SWCNTs **8** precipitate rapidly due to the predominant hydrophobic character.

After that, the morphology and dispersibility of *f*-SWCNTs **12** in water suspension was investigated by TEM microscopy. Deposits of *f*-SWCNTs **12** thereof on a TEM grid showed that the functionalized SWCNTs **12** are present in small dispersed bundles and individually separated nanotubes with an average diameter of 8 nm as shown in Figure 1B, while the *p*-SWCNTs appear like meshed bundles as shown in Figure 1A. This observation supports and emphasizes the chemical functionalization and, therefore, the debundling effect. In addition, the appearance of molecular clusters in the form of black spots on the SWCNT surface after the addition of a contrast agent (2% uranyl acetate in water) in TEM observations indicates the successful covalent attachment of chemical species to the SWCNT sidewalls (Figure 1C). As shown by



**Scheme 3** Functionalization of SWCNTs using Tour reaction. (a) Isoamyl nitrite, *o*-dichlorobenzene, acetonitrile, 60°C, 19 h; (b) trifluoroacetic acid, dichloromethane, 18 h.

**Abbreviation:** SWCNTs, single-walled carbon nanotubes.



**Scheme 4** Functionalization of SWCNTs with *N*-CiproBoc-TEG-succinate **3** or *N*-CiproBoc-HEG-succinate **10**. (a) 1-(3-Dimethylaminopropyl)-3-ethylcarbodiimide, diisopropylethylamine, dichloromethane, 20 h; (b) trifluoroacetic acid, dichloromethane, 21 h.

**Abbreviations:** HEG, hexaethylene glycol; SWCNT, single-walled carbon nanotubes; TEG, triethylene glycol.

TEM images, the appearance of these spots is attributed to the complexation of the uranium with the SWCNT-anchored addends bearing coordinating groups.<sup>38</sup>

The *f*-SWCNTs **12** were further characterized by Raman spectroscopy, which is a powerful tool used to track the CNT surface modification and provide structural information (degree of defects, the nanotube chirality, and the electronic type) about CNTs before and after functionalization.<sup>39,40</sup> The Raman spectra of *p*-SWCNTs and *f*-SWCNTs **12** are illustrated in Figure 2. As can be seen, the main peak in the Raman spectrum of *p*-SWCNTs is G band at  $1,585\text{ cm}^{-1}$ , which corresponds to the  $sp^2$  hybridization of CNTs, while for *f*-SWCNTs **12** the G band appears at  $1,585\text{ cm}^{-1}$  and D band at  $1,295\text{ cm}^{-1}$  that correspond to  $sp^3$  hybridization carbon. In fact, this observation is the expected result of the introduction of functional groups covalently bound to the CNT surface, where a remarkable number of  $sp^2$ -hybridized carbon atoms have been converted to  $sp^3$  hybridization.

The spectrum of *p*-SWCNTs exhibits an absence in the D band while the spectrum of *f*-SWCNTs **12** exhibits an appearance of the D band and an increased intensity of the D band ( $I_D$ ) relative to that of the G band ( $I_G$ ) at  $1,295\text{ cm}^{-1}$ . The intensity ratio ( $I_D/I_G$ ) was 0.17, which is in accordance with the solubility results exposed above and therefore with the functionalization degree.<sup>41</sup>

In order to determine the percentage of functionalization, TGAs were conducted. For the *f*-SWCNTs **12**, the mass loss was ~45% at  $800^\circ\text{C}$ . At the same temperature, *N*-CiproBoc-HEG-succinate **10** showed a mass loss of 90% as shown in Figure 3. Using these data, we estimate that the complete destruction of compound **10** in the aggregate would cause a mass loss of about 55%, which indicates that most of the free amine groups of SWCNT **6** are functionalized with CiproBoc-HEG-succinate **10**. Moreover, the concentration of ciprofloxacin loaded on the SWCNTs has been determined by spectrophotometry. For this purpose, a calibration curve of

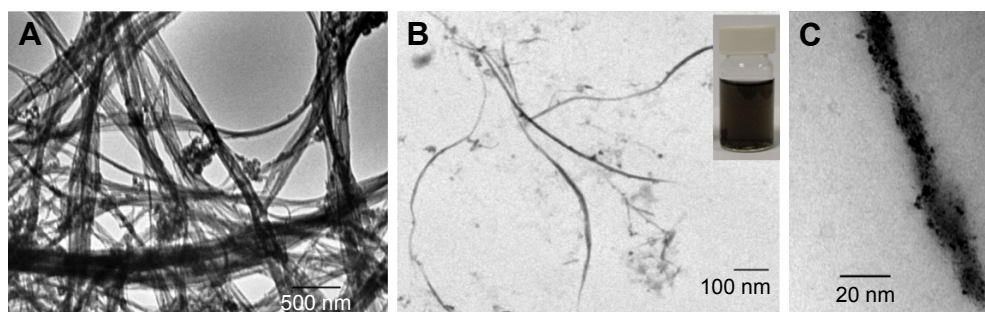


**Figure 1** TEM of (A) *p*-SWCNTs, (B) *f*-SWCNTs **12**, (inset) photograph of vial with aqueous solution of *f*-SWCNTs **12**, (C) stained *f*-SWCNTs **12** with uranyl acetate 1%.

**Abbreviations:** *f*-SWCNTs, functionalized single-walled carbon nanotubes; *p*-SWCNTs, pristine single-walled carbon nanotubes; TEM, transmission electron microscopy.

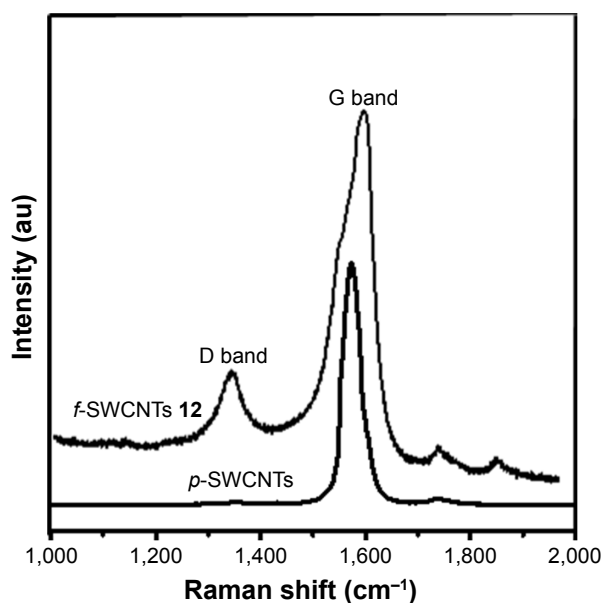


**Figure 2** Raman spectra of *p*-SWCNTs and *f*-SWCNTs **12**.

**Abbreviations:** *f*-SWCNTs, functionalized single-walled carbon nanotubes; *p*-SWCNTs, pristine single-walled carbon nanotubes.

ciprofloxacin has been constructed at  $\lambda_{\text{max}}=280$  nm, obtaining 55  $\mu\text{g}$  of ciprofloxacin/mg of *f*-SWCNTs **12**, which corresponds to the TGA results taking into account the molecular weights of compound **12** and ciprofloxacin.

In order to determine the release of the ciprofloxacin from the nanoantibiotic, an in vitro release study has been conducted using PBS at pH 7.4 in the presence of PLE and at body temperature (37°C). About 90% of the loaded ciprofloxacin was released in 2.5 h at pH 7.4. However, a detailed analysis of drug release revealed that about 30% of

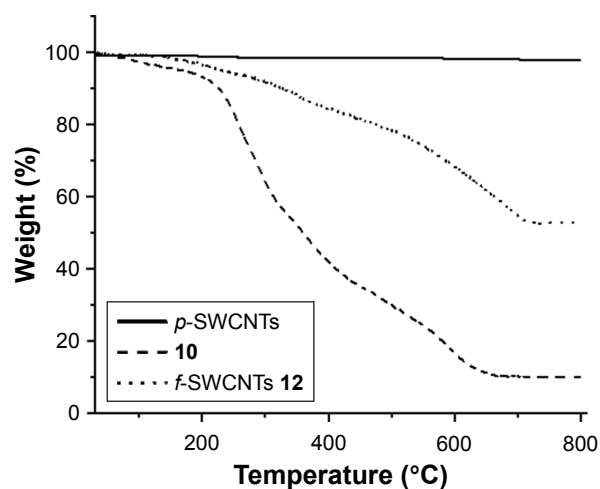


**Figure 3** TGA of *p*-SWCNTs (solid line), *f*-SWCNTs **12** (dot line), and *N*-CiproBoc-HEG-succinate **10** (dash line).

**Abbreviations:** *f*-SWCNTs, functionalized single-walled carbon nanotubes; HEG, hexaethylene glycol; *p*-SWCNTs, pristine single-walled carbon nanotubes; TGA, thermogravimetric analysis.

ciprofloxacin has been released within 20 min, and ~65% of the loaded ciprofloxacin was released after 1 h as shown in Figure 4. The analysis of the release profile can provide important information regarding the mechanisms involved in the release of the ciprofloxacin from the nanotubes. The selection of a model was based on the measure of fit of linear regression ( $R^2$ ) and the value of AIC, a measure of goodness of fit, based on maximum plausibility. For a given dataset, the most suitable model should show the lowest AIC and  $R^2$  close to 1. Among the different kinetic models that have been applied, first-order kinetics showed the best fit, since  $R^2$  was 0.997 and the AIC was about 59.<sup>32</sup> These findings are in accordance with the literature, since the selected model should demonstrate similarity between observed and predicted releases. In fact, first-order model is often used to describe the drug release profile from an ester through the hydrolysis reaction.<sup>42–44</sup>

As ciprofloxacin was successfully loaded on the surface of the SWCNTs, the antibacterial activity of the new nanoantibiotic was determined using the disc diffusion method and the MIC was measured using the broth dilution technique.

Firstly, the disc diffusion method was used to assess qualitatively the antibacterial activity of *f*-SWCNTs **12** in comparison with ciprofloxacin and *p*-SWCNTs. It was noted that there was an enhancement in the antibacterial activity for *f*-SWCNTs **12** in comparison with ciprofloxacin and *p*-SWCNTs. This was obvious from measuring the zone of inhibition for each compound against the three strains (*S. aureus*, *P. aeruginosa*, and *E. coli*). The increase in the zone of inhibition diameter indicates an increase in the antibacterial activity as can be seen in Table 1.

In a second step, the MIC of *p*-SWCNTs, ciprofloxacin, and *f*-SWCNTs **12** were determined using the broth microdilution

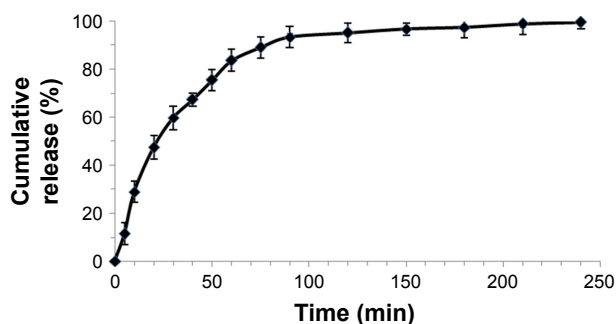


**Figure 4** In vitro release of ciprofloxacin from *f*-SWCNTs **12** in the presence of PLE up to 4 h in PBS kept at pH 7.4 and at 37°C. Values are expressed as average  $\pm$  standard deviation;  $n=3$  independent experiments.

**Abbreviations:** *f*-SWCNTs, functionalized single-walled carbon nanotubes; PLE, porcine liver esterase.



**Table 1** Results of the zone of inhibition for *f*-SWCNTs **12**, ciprofloxacin, and *p*-SWCNTs

	<i>Staphylococcus aureus</i>	<i>Pseudomonas aeruginosa</i>	<i>Escherichia coli</i>
Zone of inhibition value in cm			
<i>f</i> -SWCNTs <b>12</b>	2.9	3.8	4.8
Ciprofloxacin	2.1	2.3	4

**Abbreviations:** *f*-SWCNTs, functionalized single-walled carbon nanotubes; *p*-SWCNTs, pristine single-walled carbon nanotubes.

method. The antibacterial activity of *f*-SWCNTs **12** was higher than that of ciprofloxacin by 16 folds against *S. aureus* and *P. aeruginosa* and by 8 folds against *E. coli* while no observed antibacterial activity for *p*-SWCNTs was detected as shown in Table 2. This improvement is most likely due to the aggregation of bacteria with the SWCNTs, which in turn increased the exposure of bacteria to ciprofloxacin and, consequently, increased the concentration of ciprofloxacin that entered into bacteria. In addition, this nanoantibiotic will impair the efflux pump mechanism used by bacteria as mechanism of resistance to antibiotics as reported by Yang et al who investigated the effect of length of SWCNTs on their antimicrobial activity and reported that the longer the SWCNTs the stronger was the antimicrobial activity due to their improved aggregation with bacterial cells.<sup>45,46</sup>

Finally, the biocompatibility of the synthesized nanoantibiotic was evaluated by studying the cytotoxicity on two human cell lines and hemolysis activity on human RBCs. The cytotoxicity of the prepared nanoantibiotic was investigated on HeLa and LX2 cell lines using MTS assay. Figure 5A shows the dose–response behavior after 24 h exposure. As can be observed, there is a slight difference in the cell viability without any statistical significance ( $p$ -value >0.05), which proves the cytocompatibility of the synthesized nanoantibiotic.

One of the important aspects for the in vivo application of nanomaterials is the hemocompatibility, as the injected nanomaterials interact firstly with RBCs before the immune cells. Therefore, the hemolysis assay is considered an important feature for preclinical study. Canapè et al have reported the hemocompatibility of the functionalized SWCNTs in

**Table 2** MIC of *f*-SWCNTs **12** compared to that of ciprofloxacin

	<i>f</i> -SWCNTs <b>12</b> ( $\mu\text{g/mL}$ )	Ciprofloxacin ( $\mu\text{g/mL}$ )	Folds
<i>Staphylococcus aureus</i>	0.032	0.5	16
<i>Pseudomonas aeruginosa</i>	0.032	0.5	16
<i>Escherichia coli</i>	0.002	0.016	8

**Abbreviations:** *f*-SWCNTs, functionalized single-walled carbon nanotubes; MIC, minimum inhibitory concentration.

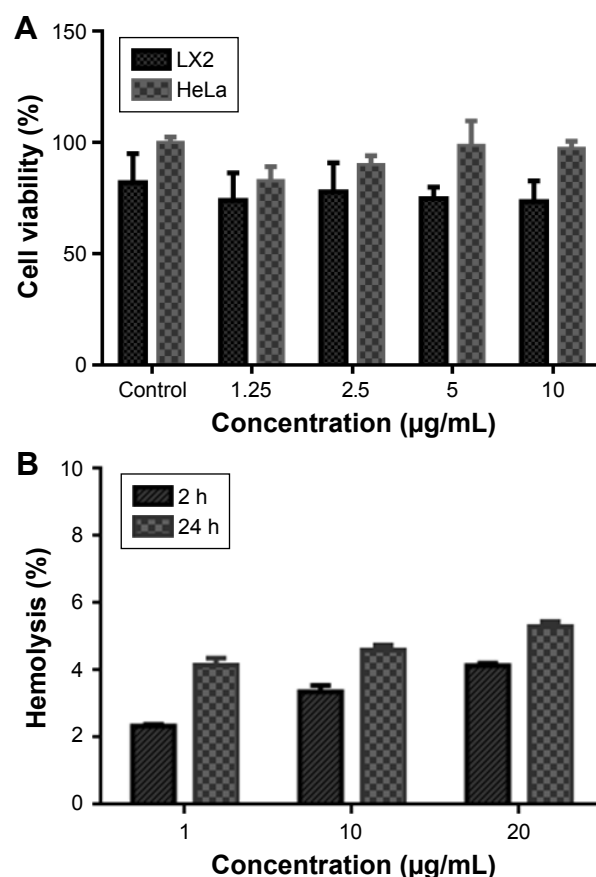


**Figure 5** (A) Cell viability assayed with the MTS assay after incubation for 24 h with the nanoantibiotic. (B) Hemolytic activity of the nanoantibiotic on RBCs after incubation times of 2 and 24 h.

**Abbreviation:** RBCs, red blood cells.

human and rat RBCs.<sup>47</sup> Herein, the hemolytic activity of the developed nanoantibiotic was studied. Figure 5B shows the percentage of hemolysis at three concentrations (1, 10, and 20  $\mu\text{g/mL}$ ) after 2 and 24 h. It appears that there is no hemolytic activity of all tested concentrations for up to 24 h with a hemolysis percentage <10% as indicated in the literature.<sup>35</sup> All used concentrations were above the MIC of the developed nanoantibiotic with a negligible hemolytic activity associated with cellular biocompatibility that favors their use for in vivo applications.

## Conclusion

The desired nanoantibiotic **12** was successfully synthesized using the radical reaction to obtain a highly stable nanoantibiotic covalently linked with ciprofloxacin through adequate hydrophilic spacer, HEG. The *f*-SWCNTs **12** showed a good dispersibility and physical stability in water for more than 6 months. Moreover, our nanoantibiotic was characterized by various analytical techniques such as TEM, Raman, and TGA. The TGA and the spectrophotometric techniques confirmed

the high loading of the ciprofloxacin on the surface of SWCNTs. The in vitro release profile showed rapid and high release of ciprofloxacin within 2.5 h at 37°C and pH 7.4 in the presence of the esterase enzyme. Most importantly, the antibacterial activity was improved significantly in comparison to the ciprofloxacin alone against three different types of bacteria (*S. aureus*, *P. aeruginosa*, and *E. coli*) as confirmed by the disc diffusion technique and the broth dilution method. Finally, this nanoantibiotic possesses good biocompatibility as confirmed by MTS assay, and its low hemolytic activity permits its further in vivo applications.

## Acknowledgments

The authors acknowledge the Palestinian Ministry of Education and Higher Education for the financial support (project number is 100/1/2013) and Biet Jala pharmaceutical company for covering the publication fee. The authors thank Professor Ismail Warad for the TGA analysis and Professor Mousa Al-Noaimi at the Hashemite University for his collaboration in NMR measurements. The authors also thank Dr Naim Kittana for the cytotoxicity test.

## Disclosure

The authors report no conflicts of interest in this work.

## References

- Cohen ML. Changing patterns of infectious disease. *Nature*. 2000; 406(6797):762–767.
- Andersson DI, Hughes D. Antibiotic resistance and its cost: Is it possible to reverse resistance? *Nat Rev Microbiol*. 2010;8(4):260–271.
- Ray PC. Size and shape dependent second order nonlinear optical properties of nanomaterials and their application in biological and chemical sensing. *Chem Rev*. 2010;110(9):5332–5365.
- Jones MR, Osberg KD, Macfarlane RJ, Langille MR, Mirkin CA. Templated techniques for the synthesis and assembly of plasmonic nanostructures. *Chem Rev*. 2011;111(6):3736–3827.
- Gao J, Gu H, Xu B. Multifunctional magnetic nanoparticles: design, synthesis, and biomedical applications. *Acc Chem Res*. 2009;42(8):1097–1107.
- Taubes G. The bacteria fight back. *Science*. 2008;321(5887):356–361.
- Cheon J, Lee J-H. Synergistically integrated nanoparticles as multimodal probes for nanobiotechnology. *Acc Chem Res*. 2008;41(12):1630–1640.
- Hajipour MJ, Fromm KM, Akbar Ashkarran A, et al. Antibacterial properties of nanoparticles. *Trends Biotechnol*. 2012;30(10):499–511.
- Webster TJ, Taylor E. Reducing infections through nanotechnology and nanoparticles. *Int J Nanomedicine*. 2011;6:1463–1473.
- Webster TJ, Seil I. Antimicrobial applications of nanotechnology: methods and literature. *Int J Nanomedicine*. 2012;7:2767–2781.
- Huh AJ, Kwon YJ. “Nanoantibiotics”: a new paradigm for treating infectious diseases using nanomaterials in the antibiotics resistant era. *J Control Release*. 2011;156(2):128–145.
- Liu Z, Tabakman S, Welsher K, Dai H. Carbon nanotubes in biology and medicine: in vitro and in vivo detection, imaging and drug delivery. *Nano Res*. 2010;2(2):85–120.
- Eatemadi A, Daraee H, Karimkhanloo H, et al. Carbon nanotubes: properties, synthesis, purification, and medical applications. *Nanoscale Res Lett*. 2014;9(1):393–405.
- Singh S, Vardharajula S, Tiwari P, et al. Functionalized carbon nanotubes: biomedical applications. *Int J Nanomedicine*. 2012;7:5361–5374.
- Guo J, Zhang X, Li Q, Li W. Biodistribution of functionalized multi-wall carbon nanotubes in mice. *Nucl Med Biol*. 2007;34(5):579–583.
- Liu Z, Davis C, Cai W, He L, Chen X, Dai H. Circulation and long-term fate of functionalized, biocompatible single-walled carbon nanotubes in mice probed by Raman spectroscopy. *Proc Natl Acad Sci U S A*. 2008; 105(5):1410–1415.
- Liu X, Hurt RH, Kane AB. Biodurability of single-walled carbon nanotubes depends on surface functionalization. *Carbon*. 2010;48(7): 1961–1969.
- Kagan VE, Konduru NV, Feng W, et al. Carbon nanotubes degraded by neutrophil myeloperoxidase induce less pulmonary inflammation. *Nat Nanotechnol*. 2010;5(5):354–359.
- Zhang Y, Bai Y, Yan B. Functionalized carbon nanotubes for potential medicinal applications. *Drug Discov Today*. 2010;15(11–12): 428–435.
- Kim J-W, Kotagiri N. Stealth nanotubes: strategies of shielding carbon nanotubes to evade opsonization and improve biodistribution. *Int J Nanomedicine*. 2014;9(Suppl 1):85–105.
- Verbrugh H, Bsc RV, van der Wall E, et al. Prophylactic ciprofloxacin for catheter-associated urinary-tract infection. *Lancet*. 1992; 339(8799):946–951.
- Wawer MJ, Sewankambo NK, Serwadda D, et al. Control of sexually transmitted diseases for AIDS prevention in Uganda: a randomised community trial. *Lancet*. 1999;353(9152):525–535.
- Bundrick W, Heron SP, Ray P, et al. Levofloxacin versus ciprofloxacin in the treatment of chronic bacterial prostatitis: a randomized double-blind multicenter study. *Urology*. 2003;62(3):537–541.
- Fass R. Efficacy and safety of oral ciprofloxacin in the treatment of serious respiratory infections. *Am J Med*. 1987;82(4A):202–207.
- Drlica K, Zhao X. DNA gyrase, topoisomerase IV, and the 4-quinolones. *Microbiol Mol Biol Rev*. 1997;61(3):377–392.
- Assali M, Joulani M, Awwad R, et al. Facile synthesis of ciprofloxacin prodrug analogues to improve its water solubility and antibacterial activity. *ChemistrySelect*. 2016;1(6):1132–1135.
- Ali SQ, Zehra A, Naqvi BS, Shah S, Bushra R. Resistance pattern of ciprofloxacin against different pathogens. *Oman Med J*. 2010;25(4): 294–298.
- Berry LM, Wollenberg L, Zhao Z. Esterase activities in the blood, liver and intestine of several preclinical species and humans. *Drug Metab Lett*. 2009;3(2):70–77.
- Li B, Sedlacek M, Manoharan I, et al. Butyrylcholinesterase, paraoxonase, and albumin esterase, but not carboxylesterase, are present in human plasma. *Biochem Pharmacol*. 2005;70(11):1673–1684.
- Taketani M, Shii M, Ohura K, Ninomiya S, Imai T. Carboxylesterase in the liver and small intestine of experimental animals and human. *Life Sci*. 2007;81(11):924–932.
- Sarin VK, Kent SB, Tam JP, Merrifield RB. Quantitative monitoring of solid-phase peptide synthesis by the ninhydrin reaction. *Anal Biochem*. 1981;117(1):147–157.
- Zhang Y, Huo M, Zhou J, et al. DDSolver: an add-in program for modeling and comparison of drug dissolution profiles. *AAPS J*. 2010; 12(3):263–271.
- Forbes BA, Sahm DF, Weissfeld AS. *Study Guide for Bailey & Scott's Diagnostic Microbiology*. St Louis, MO: Mosby; 2007.
- Wikler M. *Performance Standards for Antimicrobial Susceptibility Testing: Seventeenth Informational Supplement*. Vol 27. Wayne, PA: CLSI; 2007.
- Amin K, Dannenfelser R-M. In vitro hemolysis: guidance for the pharmaceutical scientist. *J Pharm Sci*. 2006;95(6):1173–1176.
- Bahr JL, Yang J, Kosynkin DV, Bronikowski MJ, Smalley RE, Tour JM. Functionalization of carbon nanotubes by electrochemical reduction of aryl diazonium salts: a bucky paper electrode. *J Am Chem Soc*. 2001; 123(27):6536–6542.
- Kaiser E, Coleseott R, Bossinger C, Cook P. Color test for detection of free terminal amino groups in the solid-phase synthesis of peptides. *Anal Biochem*. 1970;34(2):595–598.

38. Richard C, Balavoine F, Schultz P, Moreau N, Mioskowski C. Immobilization of histidine-tagged proteins on functionalized carbon nanotubes. *J Bionanosci.* 2007;1(2):106–113.
39. Assali M, Leal MP, Fernández I, Romero-Gomez P, Baati R, Khiar N. Improved non-covalent biofunctionalization of multi-walled carbon nanotubes using carbohydrate amphiphiles with a butterfly-like polyaromatic tail. *Nano Res.* 2010;3(11):764–778.
40. Brown S, Jorio A, Dresselhaus M, Dresselhaus G. Observations of the D-band feature in the Raman spectra of carbon nanotubes. *Phys Rev B.* 2001;64(7):073403–073406.
41. Graupner R. Raman spectroscopy of covalently functionalized single-wall carbon nanotubes. *J Raman Spectr.* 2007;38(6):673–683.
42. Mahfouz NM, Aboul-Fadl T, Diab AK. Metronidazole twin ester prodrugs: synthesis, physicochemical properties, hydrolysis kinetics and antiangiogenic activity. *Eur J Med Chem.* 1998;33(9):675–683.
43. Deshmukh M, Chao P, Kutscher HL, Gao D, Sinko PJ. A series of  $\alpha$ -amino acid ester prodrugs of camptothecin: in vitro hydrolysis and A549 human lung carcinoma cell cytotoxicity. *J Med Chem.* 2010;53(3):1038–1047.
44. Wang F, Finnin J, Tait C, et al. The hydrolysis of diclofenac esters: synthetic prodrug building blocks for biodegradable drug-polymer conjugates. *J Pharm Sci.* 2016;105(2):773–785.
45. Yang C, Mamouni J, Tang Y, Yang L. Antimicrobial activity of single-walled carbon nanotubes: length effect. *Langmuir.* 2010;26(20):16013–16019.
46. Arias LR, Yang L. Inactivation of bacterial pathogens by carbon nanotubes in suspensions. *Langmuir.* 2009;25(5):3003–3012.
47. Canapè C, Foillard S, Bonafè R, Maiocchi A, Doris E. Comparative assessment of the in vitro toxicity of some functionalized carbon nanotubes and fullerenes. *RSC Adv.* 2015;5(84):68446–68453.

## Supplementary materials

### Synthesis of *N*-Boc-ciprofloxacin (1)

Ciprofloxacin (1.0 g, 3.00 mmol) was added to 40 mL mixture of water: dioxane (1:1) containing 4.5 mL 1.0 N NaOH. After that, Boc<sub>2</sub>O (1.0 g, 4.60 mmol) was added to the prepared solution and the reaction was run to completion. Three-quarters of solvent was removed under vacuum using rotary evaporator. Thirty milliliters of acetone was added. The product was filtered by suction filtration, washed by acetone extensively, and then dried under vacuum (yield 96%, 1.25 g). The product was white to pale yellow solid. Column chromatography in dichloromethane (DCM)/MeOH (20:1) was used to purify the final product. Thin-layer chromatography (TLC) was visualized using aqueous phosphomolybdic acid followed by heating. *R<sub>f</sub>*: 0.4 (DCM/MeOH 9:1). <sup>1</sup>H NMR (300 MHz, CDCl<sub>3</sub>): δ 8.78 (s, 1H, OH), 8.58 (s, 1H, CH, C2 Ar), 8.05 (d, *J* = 12.9 Hz, 1H, CH, C5 Ar), 7.38 (d, *J* = 7.2 Hz, 1H, CH, C8 Ar), 3.54 (m, 1H, CH cyclopropyl), 3.32–3.22 (m, 8H, 4CH<sub>2</sub> of piperazine ring), 1.50 (s, 9H, 3CH<sub>3</sub> Boc), 1.44–1.37 (m, 2H, CH<sub>2</sub> of cyclopropyl), 1.24–1.18 (m, 2H, CH<sub>2</sub> of cyclopropyl). <sup>13</sup>C NMR (75.5 MHz, CDCl<sub>3</sub>): δ 177.3, 167.147, 154.79, 153.89, 147.76, 146.01, 139.26, 120.47, 112.83, 108.49, 105.23, 80.60, 67.30, 50.00, 35.51, 28.63, 8.50.

### Synthesis of *N*-Boc-ciprofloxacin-triethylene glycol (2)

A measured quantity of 20 mL of dry DCM was added to CiproBoc (290.0 mg, 0.67 mmol), triethylene glycol (TEG; 200.0 mg, 1.33 mmol), dimethylaminopyridine (DMAP; 82.0 mg, 0.67 mmol), and EDC (510.0 mg, 2.66 mmol) that were dried under N<sub>2</sub>. The reaction mixture was run for 24 h at room temperature. The reaction was extracted with 30 mL of saturated NaCl and 50 mL of DCM, and the aqueous phase was washed with DCM (2×30 mL). Na<sub>2</sub>SO<sub>4</sub> was used to dry the collected organic phase and then filtered and evaporated. Column chromatography in DCM/MeOH (20:1) was used to purify the final product. (Yield 68%, 250.0 mg, yellowish white oil). *R<sub>f</sub>*: 0.35 (DCM/MeOH 9:1). <sup>1</sup>H NMR (300 MHz, CDCl<sub>3</sub>): δ 8.58 (s, 1H, CH, C2 Ar), 8.04 (d, *J* = 12.20 Hz, 1H, CH, C5 Ar), 7.30 (m, 1H, CH, C8 Ar), 4.51 (s, 2H, COOCH<sub>2</sub>), 3.91–3.62 (m, 14H, 2CH<sub>2</sub> piperazine, 5CH<sub>2</sub> TEG), 3.45 (s, 1H, CH cyclopropyl), 3.24 (s, 4H, 2CH<sub>2</sub> piperazine), 1.5 (s, 9H, 3CH<sub>3</sub> Boc), 1.34 (d, *J* = 9.20 Hz, 4H, 2CH<sub>2</sub>, cyclopropyl). <sup>13</sup>C NMR (75.5 MHz, CDCl<sub>3</sub>): δ 164.61, 153.62, 153.37, 151.39, 147.60, 143.54, 143.56, 136.99, 122.23, 122.17, 112.51, 112.34, 108.97, 103.98, 79.20, 71.75, 69.71, 69.19, 68.21, 62.87, 60.70, 33.60, 28.68, 27.41, 7.15.

### Synthesis of *N*-Boc-ciprofloxacin-triethylene glycol-succinate (3)

A measured quantity of 20 mL of dry DCM was added to *N*-CiproBoc-TEG 2 (200.0 mg, 0.37 mmol), succinic anhydride (74.0 mg, 0.74 mmol), triethylamine (102 μL, 0.74 mmol) that were dried under vacuum and N<sub>2</sub>. The reaction mixture was run overnight at room temperature. The reaction was extracted with 30 mL of 1.0 M HCl and 50 mL of DCM. The aqueous phase was washed with DCM (2×30 mL). The collected organic layers were dried over Na<sub>2</sub>SO<sub>4</sub>, filtered, and evaporated. The final product was purified by column chromatography in DCM/MeOH (20:1). (Yield 42%, 100 mg, yellowish oil). *R<sub>f</sub>*: 0.3 (DCM/MeOH 9:1). <sup>1</sup>H NMR (300 MHz, CDCl<sub>3</sub>): δ 8.50 (s, 1H, CH, C2 Ar), 8.12 (d, *J* = 12.20 Hz, 1H, CH, C5 Ar), 7.40 (m, 1H, CH, C8 Ar), 4.60 (s, 4H, CH<sub>2</sub>OCO), 3.97–3.72 (m, 14H, 2CH<sub>2</sub> piperazine, 5CH<sub>2</sub> TEG), 3.55 (s, 1H, CH cyclopropyl), 3.34 (s, 4H, 2CH<sub>2</sub> piperazine), 2.68 (m, 4H, 2CH<sub>2</sub>, COCH<sub>2</sub>CH<sub>2</sub>CO), 1.59 (s, 9H, 3CH<sub>3</sub> Boc), 1.44 (d, *J* = 9.20 Hz, 4H, 2CH<sub>2</sub>, cyclopropyl). <sup>13</sup>C NMR (75.5 MHz, CDCl<sub>3</sub>): δ 175.22, 174.70, 164.61, 153.62, 153.37, 151.39, 147.60, 143.54, 143.56, 136.99, 122.23, 122.17, 112.51, 112.34, 108.97, 103.98, 79.20, 71.75, 69.71, 69.19, 68.21, 62.87, 60.70, 33.60, 29.20, 28.98, 28.68, 27.41, 7.15.

### Synthesis of 4-[(*N*-Boc)aminomethyl]aniline (4)

4-Nitrobenzylamine hydrochloride (400.0 mg, 2.12 mmol) was dissolved in 12 mL of water/dioxane (1:1) and 15 mL of 1.0 N NaOH. Then, Boc<sub>2</sub>O (508.0 mg, 2.33 mmol) was added to this solution. The reaction mixture was stirred overnight at room temperature. The reaction was filtered by suction filtration and dried. The final product was purified by column chromatography in Hex/EtOAc (3:1) to obtain 4-nitrobenzyl-Boc-amine. (Yield 59%, 315.0 mg, white oil). *R<sub>f</sub>*: 0.38 (Hex/EtOAc 3:1). <sup>1</sup>H NMR (300 MHz, CDCl<sub>3</sub>): δ 7.20 (d, *J* = 8.2 Hz, 2H, 2CH, Ar), 6.76 (d, *J* = 8.6 Hz, 2H, 2CH, Ar), 4.88 (bs, 1H, NH), 3.71 (bs, 2H, CH<sub>2</sub>Ar), 1.48 (s, 9H, 3CH<sub>3</sub> Boc). <sup>13</sup>C NMR (75.5 MHz, CDCl<sub>3</sub>): δ 155.64, 145.06, 128.50, 128.09, 121.83, 84.75, 45.10, 27.52. After that, 30 mg of palladium on carbon (10%) was added to a solution of the previously obtained product (300.0 mg, 1.19 mmol) in 20 mL of acidic ethanol (by adding 20 drops of 1.0 M HCl). The reaction mixture was stirred overnight at room temperature under H<sub>2</sub> (1 bar). The reaction was extracted with 30 mL of saturated NaHCO<sub>3</sub> and 50 mL of DCM. The aqueous phase was washed with DCM (2×30 mL). The organic phase was dried over Na<sub>2</sub>SO<sub>4</sub>, filtered, and evaporated. The final product



was purified by column chromatography in Hex/EtOAc (2:1). (Yield 81%, 215 mg, white oil).  $R_f$ : 0.3 (Hex/EtOAc 2:1).  $^1\text{H}$  NMR (300 MHz,  $\text{CDCl}_3$ ):  $\delta$  7.10 (d,  $J=8.1$  Hz, 2H, 2CH, Ar), 6.66 (d,  $J=8.4$  Hz, 2H, 2CH, Ar), 4.70 (bs, 1H, NH), 4.11 (d,  $J=5.4$  Hz, 2H,  $\text{NH}_2$ ), 3.71 (bs, 2H,  $\text{CH}_2\text{Ar}$ ), 1.46 (s, 9H,  $3\text{CH}_3$  Boc).  $^{13}\text{C}$  NMR (75.5 MHz,  $\text{CDCl}_3$ ):  $\delta$  156.64, 145.86, 128.00, 127.91, 115.83, 80.75, 43.12, 28.72.

### Synthesis of *N*-Boc-ciprofloxacin-hexaethylene glycol (9)

A measured quantity of 20 mL of dry DCM was added to *N*-Boc-ciprofloxacin 1 (380.0 mg, 0.89 mmol), hexaethylene glycol (500.0 mg, 1.77 mmol), DMAP (108.0 mg, 0.89 mmol), and EDC (680.0 mg, 3.54 mmol). The reaction was allowed to run overnight at room temperature under argon. The reaction was extracted with 30 mL of saturated NaCl and 50 mL of DCM; the aqueous layer was washed with DCM (2×30 mL). The collected organic layers were dried over  $\text{Na}_2\text{SO}_4$ , filtered, and evaporated. The final product was purified by column chromatography in DCM/MeOH (20:1). (Yield 68%, 400.0 mg of yellowish white oil).  $R_f$ : 0.29 (DCM/MeOH 9:1).  $^1\text{H}$  NMR (300 MHz,  $\text{CDCl}_3$ ):  $\delta$  8.46 (s, 1H, C2 Ar), 7.97 (d,  $J=13.0$  Hz, 1H, C5 Ar), 7.22–7.19 (m, 1H, C8 Ar), 4.40 (t,  $J=13$  Hz, 1H, CH of cyclopropyl), 3.78–3.52 (m, 24H,  $12\text{CH}_2$ ), 3.16–3.13 (m, 4H,  $2\text{CH}_2$  of piperazine ring), 2.87 (bs, 4H,  $2\text{CH}_2$  of piperazine ring), 1.43 (s, 9H,  $3\text{CH}_3$  Boc), 1.27 (d,  $J=6.4$  Hz, 2H,  $\text{CH}_2$  of cyclopropyl), 1.07 (bs, 2H,  $\text{CH}_2$  of cyclopropyl).  $^{13}\text{C}$  NMR (75.5 MHz,

$\text{CDCl}_3$ ):  $\delta$  164.18, 153.61, 127.47, 136.99, 112.29, 109.07, 104.01, 79.21, 76.40, 75.77, 71.80, 69.58, 69.38, 69.11, 68.16, 62.76, 60.56, 33.55, 27.41, 7.18.

### Synthesis of *N*-Boc-ciprofloxacin-hexaethylene glycol-succinate (10)

To *N*-CiproBoc-HEG 9 (320.0 mg, 0.46 mmol), succinic anhydride (92.0 mg, 0.92 mmol), triethylamine (128  $\mu\text{L}$ , 0.92 mmol) dried under vacuum, and  $\text{N}_2$ , 20 mL of dry DCM was added. The reaction mixture was stirred overnight at room temperature. The reaction was extracted with 30 mL of 1.0 M HCl and 50 mL of DCM. The aqueous layer was washed with DCM (2×30 mL). The collected organic layers were dried over  $\text{Na}_2\text{SO}_4$ , filtered, and evaporated. The final product was purified by column chromatography in DCM/MeOH (20:1). (Yield 50%, 180 mg of yellowish oil).  $R_f$ : 0.25 (DCM/MeOH 9:1).  $^1\text{H}$  NMR (300 MHz,  $\text{CDCl}_3$ ):  $\delta$  8.49 (s, 1H, C2 Ar), 8.00 (d,  $J=13.2$  Hz, 1H, C5 Ar), 7.22 (m, 1H, C8 Ar), 4.40–4.38 (m, 1H, CH of cyclopropyl), 4.20–4.16 (m, 2H,  $\text{CH}_2\text{OCO}$ ), 3.78–3.76 (m, 2H,  $\text{CH}_2\text{OCO}$ ), 3.78–3.52 (m, 20H,  $10\text{CH}_2$ ), 3.37 (bs, 4H,  $\text{COCH}_2\text{CH}_2\text{CO}$ ), 3.16–3.14 (m, 4H,  $2\text{CH}_2$  of piperazine ring), 2.58 (d,  $J=3.4$  Hz, 4H,  $2\text{CH}_2$  of piperazine ring), 1.43 (s, 9H,  $3\text{CH}_3$  Boc), 1.27 (d,  $J=6.4$  Hz, 2H,  $\text{CH}_2$  of cyclopropyl), 1.08 (d,  $J=2.4$  Hz, 2H,  $\text{CH}_2$  of cyclopropyl).  $^{13}\text{C}$  NMR (75.5 MHz,  $\text{CDCl}_3$ ):  $\delta$  211.14, 174.09, 172.34, 171.20, 164.35, 153.65, 112.63, 112.43, 103.97, 79.28, 69.65, 69.50, 69.42, 67.97, 62.80, 60.54, 60.43, 33.64, 32.08, 28.56, 28.46, 27.41, 7.18.

#### International Journal of Nanomedicine

#### Publish your work in this journal

The International Journal of Nanomedicine is an international, peer-reviewed journal focusing on the application of nanotechnology in diagnostics, therapeutics, and drug delivery systems throughout the biomedical field. This journal is indexed on PubMed Central, MedLine, CAS, SciSearch®, Current Contents®/Clinical Medicine,

Submit your manuscript here: <http://www.dovepress.com/international-journal-of-nanomedicine-journal>

#### Dovepress

Journal Citation Reports/Science Edition, EMBase, Scopus and the Elsevier Bibliographic databases. The manuscript management system is completely online and includes a very quick and fair peer-review system, which is all easy to use. Visit <http://www.dovepress.com/testimonials.php> to read real quotes from published authors.